JACS
JOURNAL OF THE AMERICAN CHEMICAL SOCIETY

COMMUNICATION

pubs.acs.org/JACS

Self-Organizing Surface-Initiated Polymerization: Facile Access to Complex Functional Systems

Naomi Sakai,*[,†] Marco Lista,[†] Oksana Kel,[‡] Shin-ichiro Sakurai,[†,§] Daniel Emery,[†] Jiri Mareda,[†] Eric Vauthey,[‡] and Stefan Matile*[,†]

[†]Department of Organic Chemistry and [‡]Department of Physical Chemistry, University of Geneva, Geneva 1211, Switzerland

Supporting Information

ABSTRACT: Facile access to complex systems is crucial to generate the functional materials of the future. Herein, we report self-organizing surface-initiated polymerization (SOSIP) as a user-friendly method to create ordered as well as oriented functional systems on transparent oxide surfaces. In SOSIP, self-organization of monomers and ring-opening disulfide exchange polymerization are combined to ensure the controlled growth of the polymer from the surface. This approach provides rapid access to thick films with smooth, reactivatable surfaces and long-range order with few defects and high precision, including panchromatic photosystems with oriented four-component redox gradients. The activity of SOSIP architectures is clearly better than that of disordered controls.

The construction of supramolecular functional multicomponent architectures on solid surfaces that are both oriented and ordered is a key challenge in current materials sciences and beyond.[1−19] Essential processes and motifs such as lateral self-sorting and oriented antiparallel gradients are intrinsically inaccessible by solution processing and related current methods.[19] We have recently introduced zipper assembly of double-gradient supramolecular n/p-heterojunction (SHJ) photosystems as a powerful yet less practical solution.[17] "Polymer brushes" have been around for a while as promising high-speed, low-cost alternatives.[14−16] However, they seem to stop growing well as soon as more interesting chemistry concerning organization or function is addressed. Implementing lessons from nature, we here report self-organizing surface-initiated polymerization (SOSIP) as a general method to create ordered and oriented functional systems on transparent oxide surfaces.

We thought that reversible surface-initiated polymerization of functional monomers equipped with functional subunits embedded within self-organizing subunits would afford highly ordered and oriented architectures. To test the hypothesis, initiator **1** and propagators **2**−**6** were designed and synthesized (Figure 1A, also see Supporting Information). As functional subunits, naphthalenediimides (NDIs) were selected. Their π-stacks can be used to transport electrons efficiently, and their color and redox properties can be changed without global structural changes.[20] As self-organizing subunits in **1** and **2**, lysine-derived diamides were envisioned to organize SOSIP architectures with networks of hydrogen bonds[17−19,21,22] around the equally organizing NDI π-stacks.[22−24]

For ring-opening surface-initiated polymerization, several candidates were screened. Reversible disulfide exchange turned out to be best. This reaction is well known from protein folding and has been used to tackle other challenges in chemistry and biology, such as lipid bilayer polymerization, dynamic molecular recognition, and mechanical bonding.[23−29] More classical methods such as ATRP[14] and ROMP,[15] as well as bio-inspired alternatives such as ring-opening thioester[30] or hydrazone exchange,[31] were more problematic in our hands. To realize SOSIP with ring-opening disulfide-exchange polymerization, protected cysteine and asparagusic acid, a strained cyclic disulfide,[27,28] were added next to the self-organizing subunits in initiator **1** and propagators such as **2**. To bind to indium tin oxide (ITO) surfaces in a well-defined orientation, initiator **1** was equipped with two diphosphonate "feet".[32] From here, SOSIP was designed to occur as follows: Reduction of the disulfides in **7** with (*S*,*S*)-dithiothreitol (DTT) liberates reactive thiolates on the surface of **8**. Recognition of propagators such as **2** on the surface of **8** by the topologically matching self-organizing and functional subunits is expected[21−24] to position the terminal disulfides of **2** on top of two thiolates on the surface of **8**. This self-organization was thus conceived to facilitate intramolecular ring-opening disulfide exchange at both termini of **2** to freeze the desired surface architecture in a covalent macrocycle.[23] At the same time, active thiolates are reproduced on the surface of intermediate **9** to react with the next propagator **2**, to continue with reversible disulfide exchange to ultimately yield the desired ladderphane[23,33] polymer brush architecture **10**.

Microcontact printing (μCP) was used to prove the occurrence of SOSIP.[34] An ITO surface was patterned with initiator **1** (Figure 2A), activated with DTT, and incubated with **2** and iPr$_2$NEt as a base catalyst under optimized conditions (see below). AFM images demonstrated that polymerization occurred exclusively on activated surfaces (Figure 2B).

SOSIP was strongly dependent on the nature and concentration of propagators **2**−**6** and the base catalyst (Figures S5 and S6). The dependence on propagator concentration was characterized by c_{SOSIP}, the critical propagator concentration needed to achieve significant SOSIP. Above c_{SOSIP}, SOSIP showed a steep nonlinear increase with propagator concentration (Figure S5). This behavior, characteristic for polymerizations, hampered quantitative reproducibility, whereas the qualitative reproducibility of SOSIP was perfect. The onset of competing polymerization in solution occurred at higher concentration, c_{SOL}. Whereas absolute

Received: April 25, 2011
Published: June 16, 2011

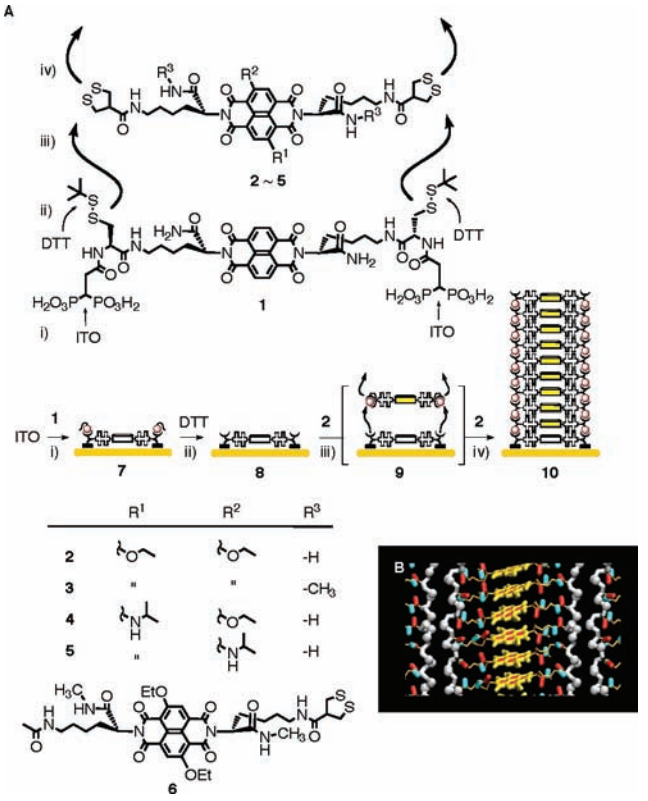

Figure 1. Design and model of SOSIP architectures with structures of initiator **1** and propagators **2**−**6**. (A) Synthesis of **10** by (i) deposition of initiator **1** on ITO, (ii) activation with DTT, self-organizing recognition of propagator **2** and ring-opening disulfide exchange (iii), for continuing SOSIP (iv). For full chemical structures, see Figure S2. Polymerization mechanisms and polymer structures are shown only to explain design strategies. They can be considered as mostly speculative but are consistent with all reported experimental data. (B) General Amber Force Field (GAFF) models of **10** (NDIs, yellow; H-bond donors, red; H-bond acceptors, blue; polymer backbone, silver).

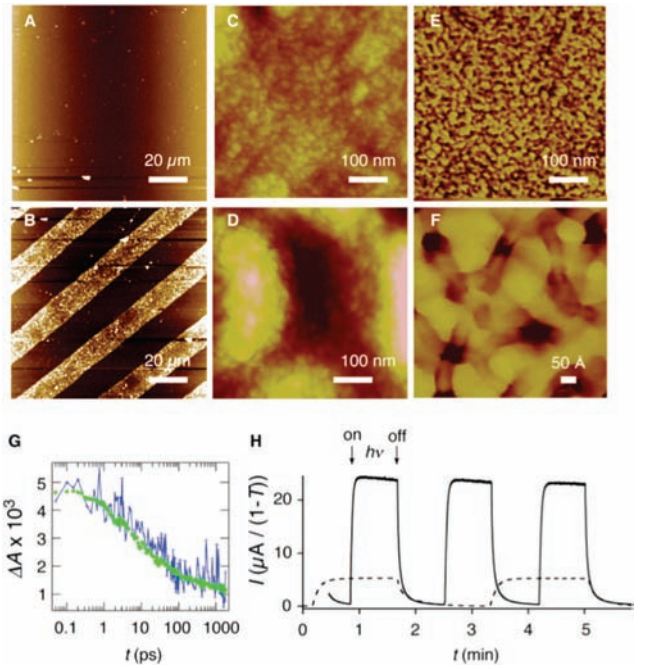

Figure 2. Comparing SOSIP architectures **10** with disorganized controls **10′** obtained by polymerization in solution. Both were made with propagator **2**. (A) AFM height image after μCP of **1** on ITO; the printed areas are not visible at the AFM detection limits. (B) μCP becomes visible by AFM after treatment with DTT and then propagator **2** (z = 0 (black)−100 nm (white)). (C) AFM height images of **10**. (D) Same for **10′** (z = 0 (black)−50 nm (white)). (E) AFM phase-contrast image of **10** (corresponding to panel C). (F) Zoom-in of panel E. (G) Transient absorption at 550 nm of **10** (green) and **10′** (blue) after excitation at 400 nm with a 100-fs laser pulse. (H) Transmittance-normalized photocurrent generated by **10** (—) and **10′** (---).

values for c_{SOSIP} and c_{SOL} varied from case to case, a significant SOSIP window $c_{SOSIP} < c < c_{SOL}$ was reproducibly found for all bis-asparagusyl propagators. Very weak polymerization found with mono-asparagusyl propagator **6** supported the importance of surface-bound and preorganized dithiolates to template the polymerization (Figure S5D).[35]

SOSIP with propagator **2**, performed in the window between c_{SOSIP} = 7 mM and c_{SOL} = 11 mM, exhibited saturation behavior with t_{50} = 6 h and a maximal NDI absorption of ~0.15 at 470 nm (Figure S4). This inactive surface could be reactivated with DTT to continue with polymerization ≥23 times (Figures S7−S9). The resulting $A_{470} \geq 0.9$ corresponds to a thickness of ~250 nm or, in an ideal SOSIP architecture, a stack of ~750 NDIs. Successful reactivation of smooth, ordered surfaces (Figure 2C,E) with DTT supported the expected vertical growth of the polymer from the surface and confirmed reversibility of the polymerization. The latter should be important for self-organization-driven self-repair[23−29,36] to minimize cross-linking and produce low-defect ladderphane[23,33] polymer brushes.

The polymeric precipitate obtained at $c > c_{SOL}$ was insoluble in all common solvents. Only small oligomers could be detected by MALDI-MS (Figure S19). Polymers could adsorb randomly on initiator-free ITO surfaces when precipitating during their synthesis at $c > c_{SOL}$ in solution. Comparison of the obtained architectures **10′** with SOSIP architectures **10** was ideal to characterize the latter, using propagator **2** in both cases (Figure 2). According to AFM images, the surface of SOSIP architectures **10** (Figure 2C, roughness R_a = 5.1 nm) was clearly smoother than that of solution-polymerized **10′** (Figure 2D, R_a = 87 nm) and not much rougher than the bare ITO surfaces used. Phase-contrast images of SOSIP architectures **10** revealed long-range order with very few defects (Figure 2E) and exceptionally high resolution (Figure 2F).

In ultrafast spectroscopy measurements, SOSIP architectures **10** and the disorganized control **10′**, both made with propagator **2**, had identical properties except for the important background noise produced by the rough surface of **10′** (Figures 2G, S12, and S18). This finding confirmed that both the long-range organization and the orientation with respect to the oxide surface account for the superior performance of SOSIP photosystem **10** compared to solution-polymerized **10′**, whereas their local structures are indistinguishable. Transient absorption spectra with SOSIP architectures (Figure S14) compared to those of photochemically generated $NDI^{-\bullet}$ [18] and $NDI^{+\bullet}$ (Figure S15) demonstrated that the yellow NDIs in architectures **10** and **10′** can function as both donors and acceptors to undergo symmetry-breaking photoinduced charge separation (PCS) (Figure S16).[37] Ultrafast nonradiative deactivation in fluorescence kinetics confirmed that PCS occurs with an average time constant of about 6 ps (Figure S12). The decay of the transient absorption of the charge-separated

dx.doi.org/10.1021/ja203792n |J. Am. Chem. Soc. 2011, 133, 15224–15227

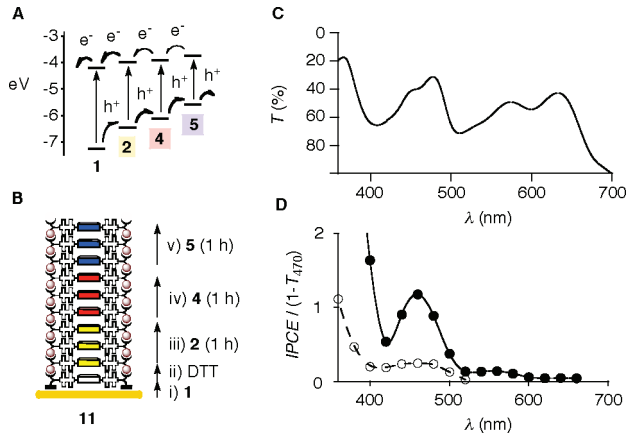

Figure 3. Panchromatic photosystems with four-component redox gradients. (A) HOMO and LUMO energies of **1**, **2**, **4**, and **5**[20] with possible electron- and hole-transfer cascades. (B) SOSIP of **11** by deposition (i) and activation (ii) of **1** on ITO followed by incubation with propagators **2** (iii), **4** (iv), and **5** (v). (C) Transmission spectrum of **11**. (D) Action spectra of multicolor photosystem **11** (●) compared to unicolor photosystem **10** (○) in transmittance-normalized IPCE (in %).

state was found to be biphasic, with lifetimes of 80 ps and >2 ns (Figures 2G and S18).

Photocurrent generation was determined with a wet setup analogue to dye-sensitized solar cells,[38,39] using SOSIP photosystems **10** as working electrode, a Pt wire counter electrode, a Ag/AgCl reference electrode, and TEOA as mobile electron carrier (Figure 2H, solid line).[17−19] Compared to disorganized photosystems **10′**, SOSIP photosytems produced about 5 times more photocurrent (Figure 2H, dashed line). Photocurrent generation by SOSIP **10** compared to control **10′** was also much faster, consistent with decreasing resistivity with increasing organization (Figure S10).

To build panchromatic SOSIP photosystems **11** with oriented four-component redox gradients, red and blue propagators **4** and **5** were designed and synthesized (Figure 3). Increasing bandgap with decreasing LUMO energies produces gradients for directional electron (e^-) transport from blue toward red, yellow, and colorless NDIs (i.e., **5**→**4**→**2**→**1**), whereas holes (h^+) could move in the other direction (i.e., **1**→**2**→**4**→**5**, Figure 3A).

With SOSIP, the construction of multicomponent photosystems **11** was very straightforward. Deposition of initiator **1** was followed by activation with DTT and incubation with yellow, red, and blue propagators **2**, **4**, and **5** for 1 h each (Figure 3B). The absorption spectrum of the panchromatic photosystem **11** demonstrated that all chromophores are incorporated in roughly equal amounts (Figure 3C). The action spectrum of multicomponent SOSIP photosystem **11** compared to that of the uniform **10** revealed that already the presence of one redox gradient suffices to increase photocurrent generation by yellow NDIs significantly (Figure 3D, ● and ○). Much poorer photocurrent generation by the red and particularly the blue NDIs in the same system indicated that these electron-rich stacks transport holes better than electrons.

Taken together, these results identify SOSIP as a user-friendly and attractive approach to oriented surface architecture with precise long-range organization. Now we are moving on to expand the approach with the introduction of more ambitious self-organizing units (i.e., $R^3 \neq H$, CH_3, Figure 1) and π-stacks used in organic solar cells to ultimately build the oriented multicolored antiparallel redox gradient (OMARG) SHJ architectures[19] needed for long-distance PCS and high efficiencies.[35,36] Preliminary results confirm that double-channel SHJ architectures obtained by co-SOSIP and self-sorting of NDI propagators already suffice to obtain at least 40 times higher activity.[40]

■ ASSOCIATED CONTENT

Supporting Information. Details on experimental procedures. This material is available free of charge via the Internet at http://pubs.acs.org.

■ AUTHOR INFORMATION

Corresponding Author

stefan.matile@unige.ch; naomi.sakai@unige.ch

Present Addresses

[§]Institute for Materials Chemistry and Engineering, Kyushu University, Fukuoka, Japan

■ ACKNOWLEDGMENT

We thank D. Jeannerat, A. Pinto, and S. Grass for NMR measurements, the Sciences Mass Spectrometry (SMS) platform for mass spectrometry services, P. Maroni and M. Borkovec for access to and assistance with surface analytics equipment, D.-H. Tran for contributions to synthesis, and the University of Geneva, the European Research Council (ERC Advanced Investigator, S.M.), the National Centre of Competence in Research (NCCR) Chemical Biology (S.M.), the NCCR MUST (E.V.), and the Swiss NSF for financial support (S.M., E.V.).

■ REFERENCES

(1) Würthner, F.; Meerholz, K. *Chem.—Eur. J.* **2010**, *16*, 9366–9373.
(2) Bassani, D. M.; Jonusauskaite, L.; Lavie-Cambot, A.; McClenaghan, N. D.; Pozzo, J.-L.; Ray, D.; Vives, G. *Coord. Chem. Rev.* **2010**, *254*, 2429–2445.
(3) Hizume, Y.; Tashiro, K.; Charvet, R.; Yamamoto, Y.; Saeki, A.; Seki, S.; Aida, T. *J. Am. Chem. Soc.* **2010**, *132*, 6628–6629.
(4) Jonkheijm, P.; Stutzmann, N.; Chen, Z.; de Leeuw, D. M.; Meijer, E. W.; Schenning, A. P. H. J.; Würthner, F. *J. Am. Chem. Soc.* **2006**, *128*, 9535–9540.
(5) Sugiyasu, K.; Kawano, S.; Fujita, N.; Shinkai, S. *Chem. Mater.* **2008**, *20*, 2863–2865.
(6) Kira, A.; Umeyama, T.; Matano, Y.; Yoshida, K.; Isoda, S.; Park, J. K.; Kim, D.; Imahori, H. *J. Am. Chem. Soc.* **2009**, *131*, 3198–3200.
(7) Martinson, A. B. F.; Massari, A. M.; Lee, S. J.; Gurney, R. W.; Splan, K. E.; Hupp, J. T.; Nguyen, S. T. *J. Electrochem. Soc.* **2006**, *153*, A527–A532.
(8) Bu, L.; Guo, X.; Yu, B.; Qu, Y.; Xie, Z.; Yan, D.; Geng, Y.; Wang, F. *J. Am. Chem. Soc.* **2009**, *131*, 13242–13243.
(9) Morisue, M.; Yamatsu, S.; Haruta, N.; Kobuke, Y. *Chem.—Eur. J.* **2005**, *11*, 5563–5574.
(10) Wasielewski, M. R. *Acc. Chem. Res.* **2009**, *42*, 1910–1921.
(11) Thompson, B. C.; Fréchet, J. M. J. *Angew. Chem., Int. Ed.* **2008**, *47*, 58–77.
(12) Bottari, G.; de la Torre, G.; Guldi, D. M.; Torres, T. *Chem. Rev.* **2010**, *110*, 6768–6816.
(13) Segura, J. L.; Martín, N.; Guldi, D. M. *Chem. Soc. Rev.* **2005**, *34*, 31–47.
(14) Snaith, H. J.; Whiting, G. L.; Sun, B. Q.; Greenham, N. C.; Huck, W. T. S.; Friend, R. H. *Nano Lett.* **2005**, *5*, 1653–1657.

(15) Weck, M.; Jackiw, J. J.; Rossi, R. R.; Weiss, P. S.; Grubbs, R. H. *J. Am. Chem. Soc.* **1999**, *121*, 4088–4089.
(16) Foster, S.; Finlayson, C. E.; Keivanidis, P. E.; Huang, Y.; Hwang, I.; Friend, R. H.; Otten, M. B. J.; Lu, L.; Schwartz, E.; Nolte, R. J. M.; Rowan, A. E. *Macromolecules* **2009**, *42*, 2023–2030.
(17) Sakai, N.; Sisson, A. L.; Bürgi, T.; Matile, S. *J. Am. Chem. Soc.* **2007**, *129*, 15758–15759.
(18) Kishore, R. S. K.; Kel, O.; Banerji, N.; Emery, D.; Bollot, G.; Mareda, J.; Gomez-Casado, A.; Jonkheijm, P.; Huskens, J.; Maroni, P.; Borkovec, M.; Vauthey, E.; Sakai, N.; Matile, S. *J. Am. Chem. Soc.* **2009**, *131*, 11106–11116.
(19) Sakai, N.; Bhosale, R.; Emery, D.; Mareda, J.; Matile, S. *J. Am. Chem. Soc.* **2010**, *132*, 6923–6925.
(20) Sakai, N.; Mareda, J.; Vauthey, E.; Matile, S. *Chem. Commun.* **2010**, *46*, 4225–4237.
(21) Pal, A.; Karthikeyan, S.; Sijbesma, R. P. *J. Am. Chem. Soc.* **2010**, *132*, 7842–7843.
(22) Molla, M.; R. Das, A.; Ghosh, S. *Chem.—Eur. J.* **2010**, *16*, 10084–10093.
(23) Shaller, A. D.; Wang, W.; Gan, H.; Li, A. D. Q. *Angew. Chem., Int. Ed.* **2008**, *47*, 7705–7709.
(24) Cougnon, F. B. L.; Au-Yeung, H. Y.; Pantos, G. D.; Sanders, J. K. M. *J. Am. Chem. Soc.* **2011**, *133*, 3198–3207.
(25) Carnall, J. M. A.; Waudby, C. A.; Belenguer, A. M.; Stuart, M. C. A.; Peyralans, J. J.-P.; Otto, S. *Science* **2010**, *327*, 1502–1506.
(26) von Delius, M.; Geertsema, E. M.; Leigh, D. A. *Nat. Chem.* **2010**, *2*, 96–101.
(27) Sadownik, A.; Stefely, J.; Regen, S. L. *J. Am. Chem. Soc.* **1986**, *108*, 7789–7791.
(28) Singh, R.; Whitesides, G. M. *J. Am. Chem. Soc.* **1990**, *112*, 1190–1197.
(29) Corbett, P. T.; Leclaire, J.; Vial, L.; West, K. R.; Wietor, J.; Sanders, J. K. M.; Otto, S. *Chem. Rev.* **2006**, *106*, 3652–3711.
(30) Ura, Y.; Al-Sayah, M.; Montenegro, J.; Beierle, J.; Leman, L.; Ghadiri, M. R. *Org. Biomol. Chem.* **2009**, *7*, 2878–2884.
(31) Skene, W. G.; Lehn, J.-M. *Proc. Natl. Acad. Sci. U.S.A.* **2004**, *101*, 8270–8275.
(32) Hanson, E. L.; Guo, J.; Koch, N.; Schwartz, J.; Bernasek, S. L. *J. Am. Chem. Soc.* **2005**, *127*, 10058–10062.
(33) Chou, C.; Lee, S.; Chen, C.; Biju, A. T.; Wang, H.; Wu, Y.; Zhang, G.; Yang, K.; Lim, T.; Huang, M.; Tsai, P.; Lin, K.; Huang, S.; Chen, C.; Luh, T. *J. Am. Chem. Soc.* **2009**, *131*, 12579–12585.
(34) Kumar, A.; Biebuyck, H. A.; Whitesides, G. M. *Langmuir* **1994**, *10*, 1498–1511.
(35) Preliminary results on surface-templated self-sorting during co-SOSIP corroborate the crucial importance of preorganized initiators for SOSIP.[40]
(36) Preliminary results obtained for barrier removal during self-sorting co-SOSIP of double-channel photosystems support the occurrence of self-repair during SOSIP.[40]
(37) Bhosale, S.; Sisson, A. L.; Talukdar, P.; Fürstenberg, A.; Banerji, N.; Vauthey, E.; Bollot, G.; Mareda, J.; Röger, C.; Würthner, F.; Sakai, N.; Matile, S. *Science* **2006**, *313*, 84–86.
(38) Oregan, B.; Grätzel, M. *Nature* **1991**, *353*, 737–740.
(39) Daeneke1, T.; Kwon, T.-H.; Holmes, A. B.; Duffy, N. W.; Bach, U.; Spiccia, L. *Nat. Chem.* **2011**, *3*, 211–215.
(40) Lista, M.; Areephong, J.; Sakai, N.; Matile, S. *J. Am. Chem. Soc.* **2011**10.1021/ja204020p.